Organic Electronics 38 (2016) 130–138

Contents lists available at ScienceDirect

Organic Electronics

journal homepage: www.elsevier.com/locate/orgel

Formation of poly(9,9-dioctylfluorene) β-phase by incorporating aromatic moiety in side chain

Sen Zhao, Junfei Liang, Ting Guo, Yu Wang, Xuan Chen, Denghao Fu, Junbin Xiong, Lei Ying*, Wei Yang, Junbiao Peng**, Yong Cao

Institute of Polymer Optoelectronic Materials and Devices, State Key Laboratory of Luminescent Materials and Devices, South China of University of Technology, Guangzhou 510640, China

ARTICLE INFO

Article history:
Received 12 May 2016
Received in revised form
27 July 2016
Accepted 8 August 2016

Keywords:
β-Phase
Dibenzothiophene-*S,S*-dioxide
Poly(9,9-di-*n*-octylfluorene)
High efficiency
Blue light emission

ABSTRACT

Two novel polyfluorene-based blue-light emitting copolymers consisting of aromatic carbazole or dibenzothiophene-*S,S*-dioxide (SO) moiety in side chain are designed and synthesized based on a palladium-catalyzed Suzuki polymerization. The UV–vis absorption, photoluminescence characteristics and wide-angle X-ray diffraction measurements of the resulting copolymers demonstrate that the incorporation of such aromatic units can induce the formation of the β-phase. The resulting copolymers consisting of aromatic units exhibit improved electroluminescence properties relative to the pristine PFO film. A maximum luminous efficiency of 2.25 cd A^{-1} with Commission Internationale de l'Eclairage coordinates of (0.17, 0.09) is obtained from the light-emitting device based on the copolymer consisting of SO unit (PFO-SO). Device based on copolymer PFO-SO also exhibits stable electroluminescent spectra and relatively low roll-off of luminous efficiency at high current densities. These observations indicate that the incorporation of aromatic moiety in side chain is a promising strategy to obtain stable blue-light-emitting polyfluorenes with enhanced efficiency.

1. Introduction

Polymer light-emitting diodes (PLEDs) have attracted tremendous attention due to their great potential in full-color flat-panel displays and solid-state lighting based on large area flexible substrates [1–3]. Among the reported conjugated polymers that have been utilized as the light-emitting layer for PLEDs, blue light-emitting polymers remain a great challenge owing to their relatively low luminous efficiency and spectra stability compared with the green and red light-emitting counterparts [4–7]. As one of the most extensively investigated blue light-emitting polymers, poly(9,9-di-*n*-octylfluorene) (PFO) have been regarded as a promising blue-emitting candidate which has high efficiency owing to the high photoluminescent quantum yield (PLQY), good charge transport property, appreciable thermal stability, as well as versatile molecular structures modifying strategies [8–11]. However, polyfluorenes also face a range of challenges. One of the most representative cases is the emergence of green-band during the long-term operation that can be correlated to the formation of the unanticipated excimers or keto-defect in the carbon bridge of backbone.

PFO can form various morphological features through different processing conditions [12–14]. Such morphological features can affect device performance and emission color. A well-studied case is the PFO β-phase, a phase with a planar zigzag conformation of polymer chain, which can result in an extended conjugation length [15–17]. In addition to inducing PFO β-phase through physically controlling PFO film forming conditions [18–20], the PFO β-phase can also be induced by chemically end-capping PFO chain end-groups by the electron-deficient oxadiazole and triazole moieties, which gives the enhanced color purity of blue emission associated with the improved device efficiency [21]. The PFO β-phase can also be formed by introducing ambipolar unit into the backbone of PFO [22]. By studying the morphology evolution of penta-fluorene oligomers thin film through temperature-dependent photoluminescence spectra, it is noted that the β-phase of oligofluorenes can be formed by cooling an amorphous thin-film to 80 K followed by slowly returning back to room-temperature [23]. The investigation of optoelectronic properties of oligofluorenes indicates that β-

---

* Corresponding author.
** Corresponding author.
E-mail addresses: msleiying@scut.edu.cn (L. Ying), psjbpeng@scut.edu.cn (J. Peng).

http://dx.doi.org/10.1016/j.orgel.2016.08.007
1566-1199/

phase can be formed in oligofluorenes consisting of more than 15 repeat units [24]. Recently, Xie and Huang introduced a remarkable progress in realizing polyfluorene with β-phase based on a smart molecular design strategy of utilizing supramolecular steric hindrance, which can be achieved by virtue of the introduction of hydrophobic interactions of the in-plane alkyl chains cross the steric hindrance. Of particular interest is that the thin film of the resulting copolymer PODPF exhibited excellent spectral stability without green band emission after thermal annealing at 200 °C under nitrogen and even under air [25]. Our previous study also reveals that a certain amount of β-phase can be formed by solvent vapor annealing of a blue light-emitting poly-(dibenzothiophene-*S*,*S*-dioxide-*co*-dioctyl-2,7-fluorene) (PFSO10), leading to the obviously enhanced luminous efficiency from 2.77 cd A^{-1} for the pristine device to 4.8 cd A^{-1} for device after solvent vapor treatment [19]. The β-phase of poly(9,9-dioctylfluorene) (PFO) can also be induced through addition of a high boiling-point solvent of 1-chloronaphthalene, where the improved external quantum efficiency of 1.85% associated with color purity of (0.16,0.10) can be achieved [26].

In this article, we report a novel strategy to induce the formation of β-phase in PFO film, which is carried out by chemically incorporating an electron-rich carbazole (Cz) unit as the donor moiety or electron-deficient SO unit as the acceptor moiety in side chain. It is noted that the electroluminescence (EL) performance can be remarkably improved upon the incorporation of aromatic Cz or SO unit. The champion device performance with the maximum luminous efficiency of 2.25 cd A^{-1} is achieved with the Commission Internationale de l'Eclairage (CIE) coordinates of (0.17, 0.09) for device based on polymer consists of SO unit in the side chain.

2. Results and discussion

2.1. Synthesis and characterization

The detailed synthesis of monomers and polymers is shown in Scheme 1. Compound 2-(8-bromooctyl)dibenzo[*b*,*d*]thiophene (**3**) is synthesized based on the alkylation reaction of 2-bromo-dibenzo[*b*,*d*]thiophene (**2**) and 1,8-dibromooctane at −78 °C. Compound 2-(8-bromooctyl)dibenzo[*b*,*d*]thiophene-5,5-dioxide (**4**) is prepared in a good yield of 85% based on an oxidizing reaction using hydrogen peroxide as the oxidizer. The alkylation of carbazole by 1,8-dibromooctane gives the intermediate compound 9-(8-bromooctyl)-9*H*-carbazole (**5**) in a good yield. The monomer 9-(8-(2,7-dibromo-9-octyl-9*H*-fluoren-9-yl)octyl)-9*H*-carbazole (**M1**) is synthesized based on the reaction of **4** and **5** in a good yield of 85% in the presence of sodium hydroxide. Similarly, the monomer 2-(8-(2,7-dibromo-9-octyl-9*H*-fluoren-9-yl)octyl)dibenzo-[*b*,*d*]thiophene-5,5-dioxide (**M2**) can be synthesized based on the reaction of 2,7-dibromo-9-octyl-9*H*-fluorene (**6**) and **4** in a yield of 87%. The molecular structures of the target monomers are confirmed by ^{1}H NMR and ^{13}C NMR spectra (shown in Fig. S1 and Fig. S2 in the Supporting Information).

The target polymers are synthesized based on the Suzuki polymerization, which is carried out by copolymerizing the monomer 2,7-bis-(4,4,5,5-tetramethyl-1,3,2-dioxaborolan-2-yl)-9,9-dioctylfluorene (**M3**), 2,7-dibromo-9,9-dioctylfluorene (**M4**), with 1 mol% of dibromo monomer **M1** or **M2**, with relevant copolymers denoted as PFO-Cz and PFO-SO, respectively. Both copolymers can be easily dissolved in common organic solvents, such as tetrahydrofuran (THF), chloroform ($CHCl_3$), chlorobenzene and dichlorobenzene. The number average molecular weight (M_n) estimated by gel permission chromatography (GPC) is 30.5 and 73.0 kDa, with polydispersity index (PDI) of 1.55 and 1.62 for PFO-Cz and PFO-SO, respectively. Detailed molecular weight data are summarized in Table 1.

2.2. Thermal properties

Differential scanning calorimetry (DSC) and thermal gravimetric analysis (TGA) measurements are used to evaluate the thermal properties of the resulting polymers, with relevant characteristics shown in Fig. 1. No obvious glass transition temperature can be observed during the heating process. However, it is interesting to note that copolymers PFO-Cz and PFO-SO exhibit the melting temperature (T_m) of 154 °C and 156 °C, respectively during the heating process. During the cooling procedure, one notes the crystallization temperature (T_c) of 79 °C and 83 °C for copolymers PFO-Cz and PFO-SO, respectively [8,22]. Moreover, the decomposition temperatures (T_d, corresponding to the temperature at 10% weight loss) of these copolymers are higher than 380 °C, indicating good thermal stability of these copolymers. Detailed thermal properties data are summarized in Table 1.

2.3. Photophysical properties

Fig. 2 shows the normalized UV–vis absorption and photoluminescent (PL) spectra of polymers in toluene solution with concentration of about 1×10^{-5} g mL^{-1} and as thin films. In toluene solution, the absorption profiles of both PFO-SO and PFO-Cz show the maximum absorption at about 390 nm, which can be attributed to the π-π^* transition [27]. The PL spectra of PFO-SO and PFO-Cz are quite comparable with that of PFO, which exhibit three characteristic peaks located at 415, 440 and 470 nm.

The UV–vis absorption of copolymers PFO-Cz and PFO-SO as thin films exhibit slightly broadened profiles relative to that of PFO. It is interesting to note that a new peak located at 436 nm emerged in both absorption profiles of PFO-Cz and PFO-SO, indicating the formation of PFO β-phase in such thin films. By deconvolution of the absorption spectra, the content of β-phase is determined to be about 1% and 7% for PFO-Cz and PFO-SO, respectively.

The observation of the formed β-phase can also be reflected in the corresponding PL spectra. As shown in Fig. 2b, PL profiles for these copolymers are apparently different. The PL spectrum of PFO spin-casted from toluene solution exhibits characteristic amorphous phase, with emission peaks located at 426 (0-0 band), 450 (0–1 band), and 475 nm (0–2 band). In contrast, the PL spectra of the PFO-Cz and PFO-SO show emission peaked at 440 nm (0-0 band), 462 nm (0–1 band) and 497 nm (0–2 band), which can be attributed to the PFO β-phase. The existence of PFO β-phase can also be revealed by X-ray diffraction (XRD) patterns of such thin films (see Fig. S3 in the SI). One can clearly see a characteristic peak with 2θ value of about 7.0° for both PFO-SO and PFO-Cz films, which can be correlated to the characteristic peak of PFO β-phase [8,22,28]. In contrast, the morphology of the pristine PFO film that processed under the same condition is featureless. The combination of XRD patterns and those observations of UV–vis and PL spectra confirms the formation of PFO β-phase in such thin films. While the emission of PFO-Cz exhibits obvious characteristic emission corresponding to PFO β-phase, one can still observe the existence of a slight shoulder peak located at 422 nm (0-0 band for the amorphous phase), implying the incomplete energy transfer from the amorphous phase to the β-phase of PFO. The fluorescence quantum yields (Φ_{PL}) of copolymers PFO-Cz and PFO-SO are evaluated to be 45.7% and 43.3%, respectively, which are much higher than that of 32.7% for PFO film. The optical band gap (E_g^{opt}) as estimated from the onset absorption is 3.00, 2.92 and 2.94 eV for copolymers PFO, PFO-Cz and PFO-SO, respectively. Detailed photophysical parameters are summarized in Table 2.

2.4. Electrochemical properties

Electrochemical properties of copolymers are examined by cyclic voltammetry (CV). Fig. 3 shows the *p*-doping traces of PFO, PFO-

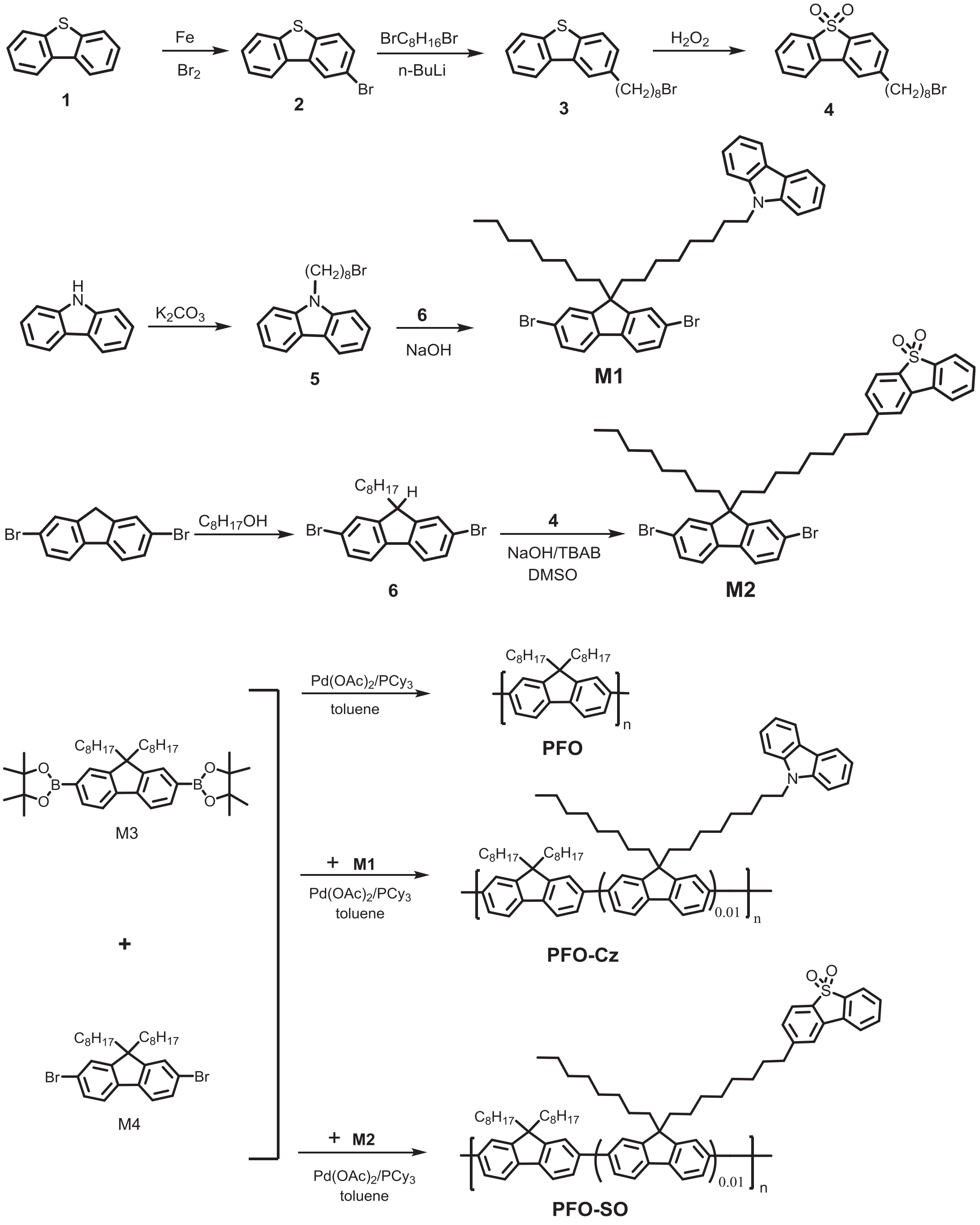

Scheme 1. Synthetic route for monomers and copolymers.

Table 1
Molecular weight and thermal properties of polymers.

Polymer	M_n (kDa)	PDI	T_c/°C	T_m/°C	T_d [a]/°C
PFO	30.5	1.51	93	156	385
PFO-Cz	65.0	1.55	79	154	396
PFO-SO	73.0	1.62	83	156	410

[a] Corresponding to 10 wt% weight loss.

Cz and PFO-SO. The oxidation potentials of polymers are calibrated by ferrocene/ferrocenium redox couple (Fc/Fc^+), which is measured to be 0.38 V. It is assumed that the redox potential of Fc/Fc^+ has an absolute energy level of 4.80 V to vacuum [26]. Therefore, the highest occupied molecular orbital (HOMO) levels of the copolymers are calculated according to the equation of $E_{HOMO} = -e(E_{ox}+ 4.80-0.38)$ (eV), where E_{ox} is the onset of the oxidation potentials relative to Ag/Ag^+. Thus, the E_{HOMO} of copolymers is calculated to be −5.83, −5.79 and −5.81 eV, respectively. Unfortunately, we failed to record any reliable n-doping process. Thus, to get the lowest unoccupied molecular orbital energy levels (E_{LUMO}) of these polymers, the E_{LUMO} is estimated based on the difference between E_{HOMO} and the optical band gap (E_g^{opt}), which is determined to be −2.83, −2.87 and −2.87 eV for copolymers PFO, PFO-Cz and PFO-SO, respectively. In considering that the small molar ratio of Cz and SO unit is attached to the PFO backbone through a non-conjugated fashion, which will not disturb

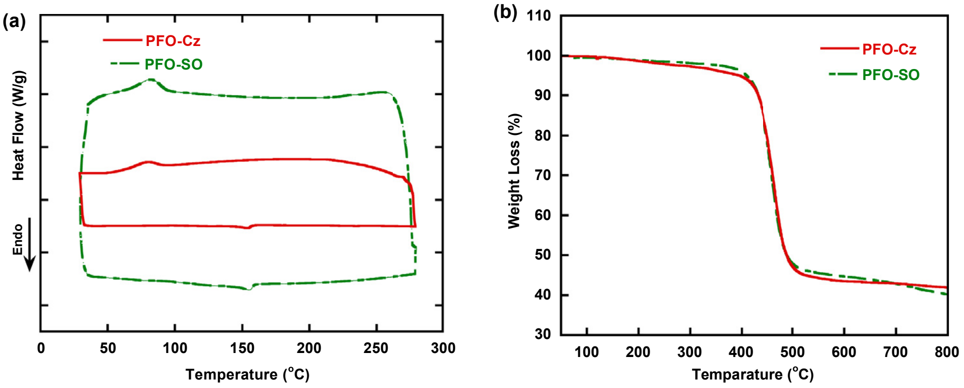

Fig. 1. DSC and TGA curves of copolymers.

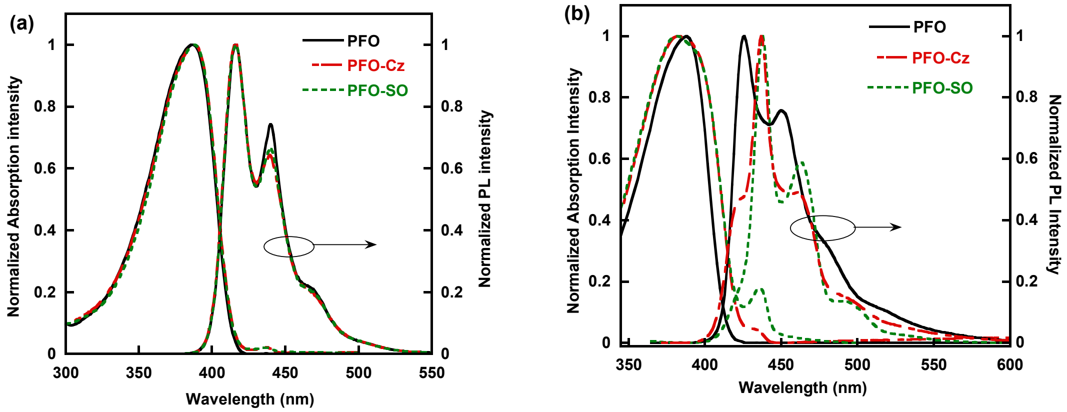

Fig. 2. UV–vis absorption and PL spectra of copolymers in toluene solution with concentration of 1 × 10^{-5} g mL^{-1} (a) and as thin films (b).

Table 2
Photophysical data and energy levels of the polymers.

Polymer	$\lambda_{max}{}^{abs}$	$\lambda_{max}{}^{PL}$	UV–vis	PL	HOMO/LUMO[a]	E_g^{opt} [b]	Φ_{PL} [c]
	In solution (nm)		As thin films (nm)		(eV)	(eV)	(%)
PFO	388	417	388	425	−5.83/−2.83	3.00	32.7
PFO-Cz	388, 436	414	383, 434	437	−5.79/−2.87	2.92	45.7
PFO-SO	389, 437	417	383, 435	437	−5.81/−2.87	2.94	43.3

[a] Estimated from the HOMO levels and optical band gaps.
[b] Onset of the absorption spectra.
[c] Measured in solid states.

the electron distribution along the polymer backbone, thus these copolymers exhibit quite comparable E_{HOMO}/E_{LUMO}. The detailed CV results are summarized in Table 2.

2.5. Electroluminescence properties

The electroluminescence of these copolymers are evaluated based on polymer light-emitting devices with configuration of ITO/PEDOT:PSS/polymer (80 nm)/CsF (1.5 nm)/Al (80 nm). Fig. 4a shows the EL spectra of these polymers. The EL spectra are quite analogous for all copolymers, with the maximum emission peaked at about 440 nm. The CIE coordinates for PFO-SO is (0.17, 0.09), which lies in deep-blue region. This high color purity in blue emission is due to the lack of apparent long-wavelength emission in the EL spectrum. We note that the emission spectra of PL and EL are different, which can be attributed to different mechanism in these process. In PL, the mechanism is Förster energy transfer. In EL, the PFO β-phase acts as the electron-trap, where the LUMO of PFO β-phase is located 0.12 eV below that of the amorphous phase [28]. Thus, the PL spectra of the resulting copolymers exhibit the combination of both

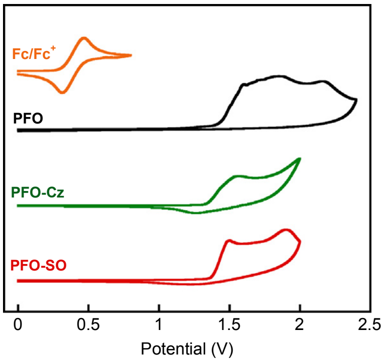

Fig. 3. CV curves of copolymers.

Table 3
EL characteristics of the copolymers.

Polymer	V_{on} (turn on)	LE_{max} (cd A^{-1})	L_{max} (cd m^{-2})	CIE (x, y)
PFO	4.6	0.6	2691	0.18, 0.17
PFO-Cz	3.4	1.4	4916	0.18, 0.10
PFO-SO	4.4	2.25	5101	0.17, 0.09

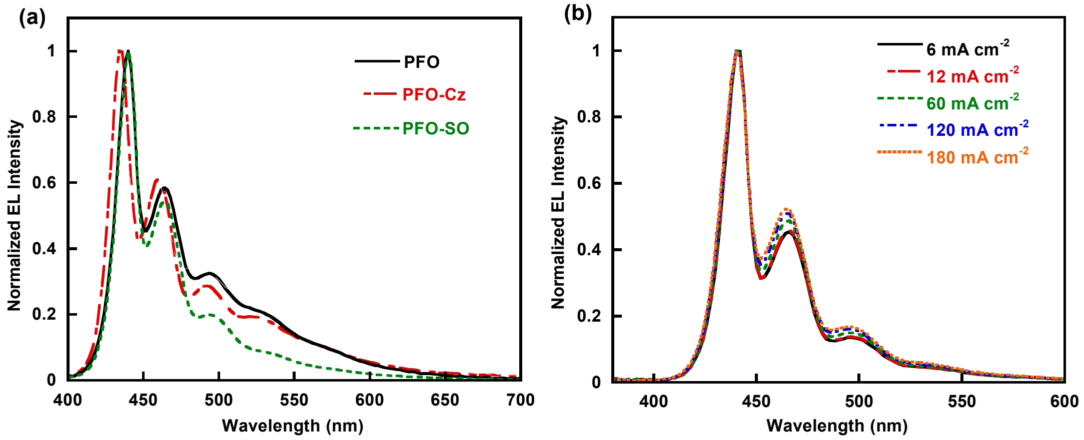

Fig. 4. EL spectra of the resultant copolymers (a) and PFO-SO at various current densities (b).

amorphous phase and β-phase, while in EL spectra, only β-phase emission is observed.

Of particular interest is that these EL spectra exhibit excellent stability under various current densities. For instance, the EL profiles remain nearly unchanged with the current density increased from 6 to 180 mA cm^{-2} for device based on PFO-SO as the emissive layer (Fig. 4b).

Fig. 5 shows the luminous efficiency (LE) as a function of current density (J) ($LE - J$) characteristics (a), and current density (J) and luminance (L) as functions as driving voltage (V) ($J - V - L$) characteristics (b) of devices based on PFO, PFO-Cz and PFO-SO. It is worth noting that both devices based on PFO-Cz and PFO-SO as the emissive layer show luminous efficiencies of 1.4 and 2.25 cd A^{-1}, respectively, both of which are much higher than that obtained from the device based on PFO as the emissive layer. Detailed electroluminescent performances of the resulting devices are summarized in Table 3. The improved performance can be attributed to the increased PL quantum efficiency of such copolymers as a result of the formation of PFO β-phase, or might be correlated to more balanced charge carrier transport in the emissive layer. We note that the obtained luminous efficiencies are relatively low, which can be attributed to the large hole injection barrier between the PEDOT:PSS (work function of -5.2 eV) and the resulting copolymer films (work function ~ -5.80 eV), leading to the inefficient hole injection that is responsible for the relative low luminous efficiencies. In this regard, it is rational to suppose that the luminous efficiency can be enhanced upon employing appropriate device structures.

Moreover, from Fig. 5b one notes that the device based on PFO-Cz shows the lowest turn on voltage of 3.4 V among these devices, and both the current density and luminance of device based on PFO-Cz is much higher than the other devices at a given driving voltage, which can be understood as that the attached electron-donating Cz unit can effectively facilitate hole injection from the anode. The incorporation of SO unit leads to the slightly decreased current density, which might be correlated to the formation of electron-trap as a result of the high content of PFO β-phase. To our knowledge, this is the first report of improving blue light-emitting efficiency and color purity of PFO by inducing the formation of β-phase through incorporating organic units into side chain as additives.

2.6. Charge carrier mobility

To investigate the effect of incorporating aromatic Cz or SO units on the charge carrier transport properties in the emissive layer, we fabricate the single charge carrier devices. The device architectures for hole- and electron-only devices are ITO/PEDOT:PSS (40 nm)/polymer (80 nm)/MoO_3 (10 nm)/Al (100 nm) and ITO/ZnO(40 nm)/polymer(80 nm)/CsF(1.5 nm)/Al(100 nm), respectively. Fig. 6 shows the characteristic $J - V$ characteristics of devices. We note that the electron mobility slightly decrease in PFO-Cz and PFO-SO films, which is understandable since the PFO β-phase is essentially electron-trap that can effectively decrease the electron flux [29]. This issue can also be confirmed since the PFO-SO film with higher content of β-phase exhibited lower electron mobility. It is also

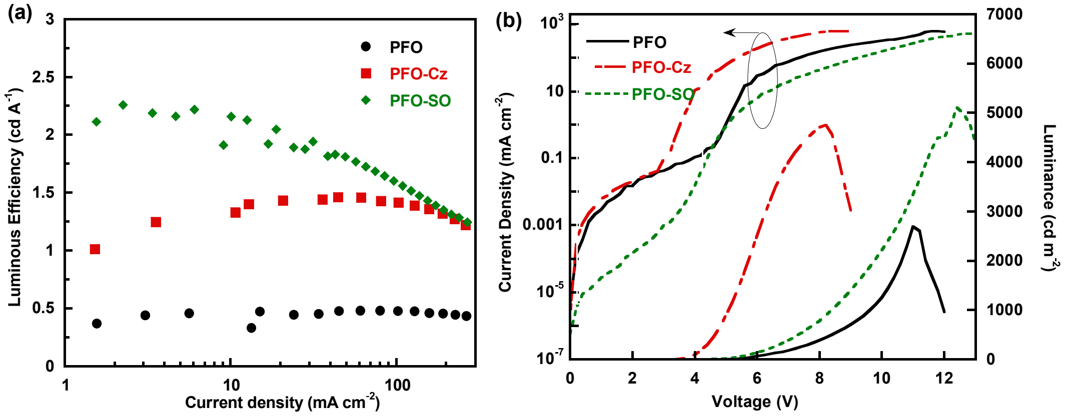

Fig. 5. $LE - J$ (a) and $J - V - L$ (b) characteristics of copolymers. Device structure: ITO/PEDOT:PSS/polymer/CsF/Al.

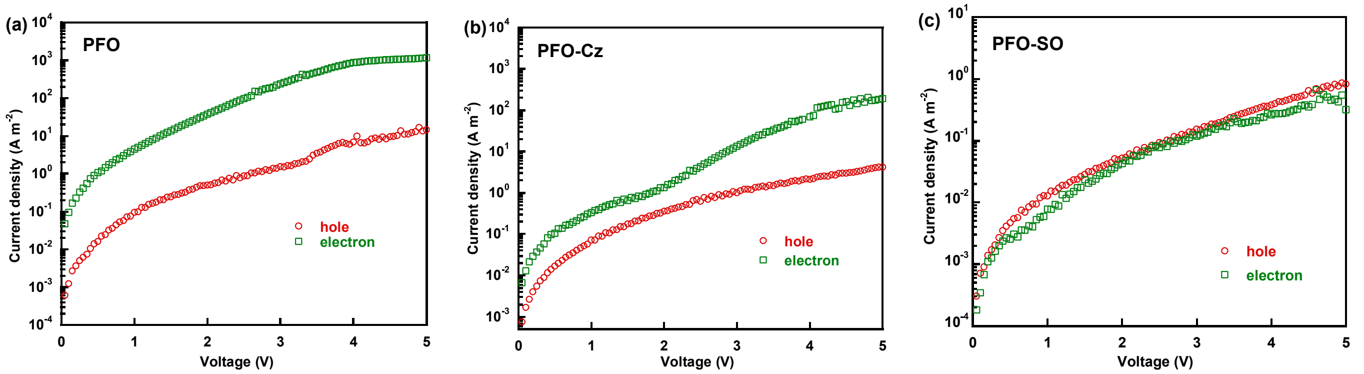

Fig. 6. Current densities as a function of driving voltage of devices based on PFO (a), PFO-Cz (b) and PFO-SO (c).

worth pointing out that the decreased electron mobility leads to more balanced charge carrier transport across the entire applied voltage range for devices based on PFO-Cz and PFO-SO than that for PFO. As shown in Fig. 6c, for device based on PFO-SO the electron and hole densities are very comparable under the same driving voltage, indicating the significantly enhanced balance of charge carrier in the emissive layer. This observation is consistent with the fact that the device based on PFO-SO exhibits the highest luminous efficiency.

2.7. *Film morphology*

Tapping mode atomic force microscopy (AFM) measurements are carried out to get insight into the effects of incorporated aromatic unit on the film morphology, with relevant images shown in Fig. 7. The films are spin-casted from toluene solution on the top of the prefabricated PEDOT:PSS layer. The PFO film exhibits quite smooth morphology with root-mean-square (RMS) value of 0.5 nm. In contrast, the films based on copolymers consisting of Cz and SO moiety in the side chains exhibit rougher morphology, with RMS values of 1.0 nm and 1.6 nm for PFO-Cz and PFO-SO, respectively. The increased roughness indicate that the incorporation of Cz and SO can induce the reorganization of PFO-Cz and PFO-SO chains. These observations associated with the obviously increased device performances highlight that the incorporation Cz or SO unit can be an effective strategy for attaining the improved blue light-emission of polyfluorenes.

3. Conclusion

In summary, two novel polyfluorene derivatives are designed and synthesized by incorporating a small amount of aromatic carbazole and dibenzothiophene-*S*,*S*-dioxide unit into the side chain of PFO. The device performance in terms of luminous efficiency and luminance can be significantly improved after the incorporation of such aromatic moieties. The enhancement of device performances can be primarily attributed to the increased fluorescence quantum yields, more balanced electron/hole flux as well as the increased roughness of film surfaces due to the formation of PFO β-phase. It is also worth pointing out that the electroluminescent spectra exhibited excellent stability even at higher current densities. These observations indicate that incorporation of a small amount of aromatic units in PFO side chain can be an effective strategy for improving the performances of blue light emitting PLEDs.

4. Experimental section

4.1. *Materials*

All manipulations involving air-sensitive reagents were performed under an atmosphere of dry argon. Toluene and THF were purified by standard procedures and distilled under dry argon before use. All reagents, unless otherwise specified, were obtained from Aldrich and Acros Chemical Co. and used as received. 2,7-dibromofluorene, 2,7-bis(4,4,5,5-tetramethyl-1,3,2-dioxaborolan-2-yl)-9,9-dioctylfluorene (**M3**), 2,7-dibromo-9,9-dioctylfluorene (**M4**) were synthesized according to reported procedures [30,31]

4.1.1. *Synthesis of monomers*

4.1.1.1. 2-Bromodibenzo[b,d]thiophene (2). Dibenzo[*b*,*d*]thiophene (11 g, 60 mmol) and iron (0.17 g, 3 mmol) were added into reaction vessel under the ice bath, then element bromine (3.1 mL, 60 mmol) was added into the reaction vessel and stirring the mixture at room temperature for 16 h. The reaction was quenched by adding sodium dithionite aqueous solution, and extracted 3 times by using dichloromethane. After removing the organic phase under reduced pressure, the crude product was purified by column chromatography with a yield of 80%. ^{1}H NMR (500 MHz, $CDCl_3$) δ (ppm) 8.27 (d, J = 1.9 Hz, 1H), 8.10 (m, 1H), 7.85 (m, 1H), 7.70 (d, J = 7.4 Hz, 1H), 7.54 (m, 1H), 7.24 (m, 2H).

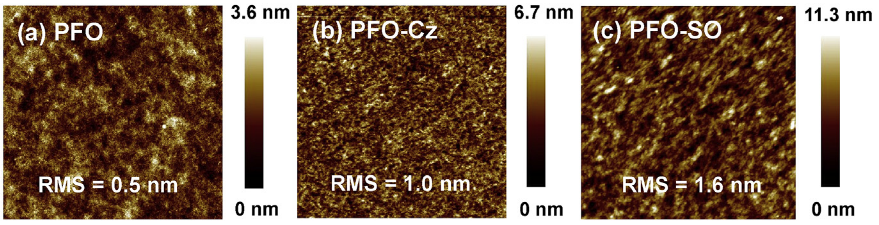

Fig. 7. AFM topography of PFO (a), PFO-Cz (b) and PFO-SO (c).

4.1.1.2. 2-(8-Bromooctyl)dibenzo[b,d]thiophene (3). 2-Bromodibenzo[*b*,*d*]thiophene (3.3 g, 12.5 mmol) was solved in dry THF under Ar atmosphere, then *n*-BuLi (3.3 g, 12.5 mmol) was added into the reaction vessel and stirring the mixture at −78 °C for 2 h, then 1,8-dibromooctane (11 g, 45 mmol) was added into the reaction vessel and stirring the mixture at −78 °C for 1 h. The reaction was quenched by adding water, and extracted 3 times by using dichloromethane. After removing the organic phase under reduced pressure, the crude product was purified by column chromatography with a yield of 70%. ^{1}H NMR (500 MHz, $CDCl_3$) δ (ppm) 8.18–8.12 (m, 1H), 7.96 (d, $J = 1.1$ Hz, 1H), 7.89–7.82 (m, 1H), 7.75 (d, $J = 7.2$ Hz, 1H), 7.48–7.42 (m, 2H), 7.29 (m, 1H), 3.41 (m, 2H), 2.86–2.74 (m, 2H), 1.85 (m, 2H), 1.71 (m, 2H), 1.49–1.28 (m, 8H). ^{13}C NMR (125 MHz, $CDCl_3$) δ (ppm) 139.97, 139.36, 136.83, 135.83, 135.66, 127.79, 126.67, 124.34, 123.00, 122.63, 121.63, 121.29, 36.12, 34.07, 32.95, 31.99, 29.47, 29.30, 28.72, 28.19.

4.1.1.3. 2-(8-Bromooctyl)dibenzo[b,d]thiophene-5,5-dioxide (4). 2-(8-Bromo-octyl)dibenzo[*b*,*d*]thiophene (5.2 g, 15 mmol) and acetic acid (40 mL) was added into reaction vessel, then H_2O_2 (8 mL) was added into reaction vessel under stirring at 120 °C. The reaction was extracted 3 times by using dichloromethane. After removing the organic phase under reduced pressure, the crude product was purified by column chromatography with a yield of 85%. ^{1}H NMR (500 MHz, $CDCl_3$) δ(ppm) 7.80 (m, 2H), 7.73 (d, $J = 7.9$ Hz, 1H), 7.63 (m, 1H), 7.58 (s, 1H), 7.52 (m, 1H), 7.33 (d, $J = 7.8$ Hz, 1H), 3.40 (t, $J = 6.8$ Hz, 2H), 2.77–2.69 (m, 2H), 2.10 (s, 2H), 1.93–1.80 (m, 2H), 1.49–1.27 (m, 8H).

4.1.1.4. 9-(8-Bromooctyl)-9H-carbazole (5). 9*H*-Carbazole (5 g, 29.9 mmol), K_2CO_3 (20.66 g, 149.52 mmol) were solved in 60 mL *N*, *N*-dimethylformamide, then the mixture was stirred for 2 h at 110 °C. Then 1,8-dibromooctane (24.40 g, 89.71 mmol) was added into reaction vessel, and stirring at 110 °C for 12 h. The mixture was extracted 3 times by using dichloromethane. After removing the organic phase under reduced pressure, the crude product was purified by column chromatography with a yield of 80%. ^{1}H NMR (500 MHz, $CDCl_3$) δ (ppm) 8.11 (d, $J = 7.7$ Hz, 2H), 7.47 (m, 2H), 7.41 (d, $J = 8.2$ Hz, 2H), 7.25–7.20 (m, 2H), 4.31 (t, $J = 7.2$ Hz, 2H), 3.38 (t, $J = 6.8$ Hz, 2H), 1.94–1.73 (m, 4H), 1.34 (m, 8H).

4.1.1.5. 2,7-Dibromo-9-octyl-9H-fluorene (6). 2,7-Dibromo-9*H*-fluorene (10 g, 30.86 mmol), KOH (860.80 mg, 15.43 mmol) and octyl alcohol (19.94 g, 154.32 mmol) were added into 250 mL reaction vessel, and stirring the mixture at room temperature for 24 h. The mixture was cooled to room temperature and vacuum distilled to remove excessive octyl alcohol. Then the mixture was extracted 3 times by using dichloromethane. After removing the organic phase under reduced pressure, the crude product was purified by column chromatography with a yield of 78%. ^{1}H NMR (500 MHz, $CDCl_3$) δ (ppm) 7.81 (d, $J = 6.4$ Hz, 2H), 7.51 (s, 1H), 7.42 (s, 1H), 7.36 (m, 2H), 4.03 (m, 1H), 2.02–2.10 (m, 2H), 1.22–1.41 (m, 12H), 0.94 (t, $J = 6.9$ Hz, 3H).

4.1.1.6. 9-(8-(2,7-Dibromo-9-octyl-9H-fluoren-9-yl)octyl)-9H-carbazole (M1). 2,7-Dibromo-9-octyl-9*H*-fluorene (5 g, 11.46 mmol), tetrabutylammonium bromide (184.75 mg, 573.10 μmol) was added into reaction vessel, then NaOH (2.29 g, 57.31 mmol) aqueous solution was added into mixture and stirring at room temperature for 2 h, 9-(8-bromooctyl)-9*H*-carbazole (4.11 g, 11.46 mmol) was added into mixture and stirring for 24 h at room temperature. The reaction was extracted 3 times by using dichloromethane. After removing the organic phase under reduced pressure, the crude product was purified by column chromatography with a yield of 85%. ^{1}H NMR (500 MHz, $CDCl_3$) δ (ppm) 8.12–8.08 (m, 2H), 7.53 (d, $J = 1.4$ Hz, 2H), 7.43 (m, 8H), 7.20 (m, 2H), 4.28 (t, $J = 7.3$ Hz, 2H), 2.76 (t, $J = 6.5$ Hz, 2H), 2.08–1.96 (m, 2H), 1.90–1.76 (m, 2H), 1.40–1.05 (m, 22H), 0.83 (t, $J = 7.2$ Hz, 3H). ^{13}C NMR (125 MHz, $CDCl_3$) δ (ppm) 148.55, 140.56, 138.66, 132.10, 127.39, 125.69, 122.94, 122.19, 121.40, 120.47, 118.81, 108.80, 87.71, 63.70, 43.21, 40.10, 31.91, 30.01, 29.83, 29.47,29.31, 29.24, 29.09, 27.42, 25.90, 23.39, 22.74, 14.22.

4.1.1.7. 2-(8-(2,7-Dibromo-9-octyl-9H-fluoren-9-yl)octyl)dibenzo[b,d]thiophene-5,5- dioxide (M2). 2,7-Dibromo-9-octyl-9*H*-fluorene (5 g, 11.46 mmol), tetra-*n*-butylammonium bromide (184.75 mg, 573.10 μmol) was added into reaction vessel, then NaOH (2.29 g, 57.31 mmol) aqueous solution was added into mixture and stirring at room temperature for 2 h, 2-(8-bromooctyl)dibenzo[*b*,*d*]thiophene 5,5-dioxide (4.67 g, 11.46 mmol) was added into mixture and stirring for 24 h at room temperature. The reaction was extracted 3 times by using dichloromethane. After removing the organic phase under reduced pressure, the crude product was purified by column chromatography with a yield of 87%. ^{1}H NMR (500 MHz, $CDCl_3$) δ (ppm) 7.81 (d, $J = 7.6$ Hz, 1H), 7.77 (d, $J = 7.7$ Hz, 1H), 7.71 (d, $J = 7.9$ Hz, 1H), 7.63 (m, 1H), 7.55 (d, $J = 0.8$ Hz, 1H), 7.54–7.49 (m, 3H), 7.46–7.42 (m, 4H), 7.29 (m, 1H), 2.83–2.50 (m, 2H), 1.95–1.84 (m, 4H), 1.58 (m, 2H), 1.23 (m, 16H), 0.83 (t, $J = 7.2$ Hz, 5H), 0.61–0.53 (m, 4H). ^{13}C NMR (125 MHz, $CDCl_3$) δ (ppm) 152.66, 150.04, 139.23, 138.42, 135.31, 133.85, 131.99, 130.68, 130.35, 130.32, 126.30, 122.30, 122.20, 121.62, 121.57, 121.30, 55.83, 40.31, 40.21, 36.32, 31.90, 31.25, 29.99, 29.86, 29.34, 29.31, 29.29, 29.12, 23.75, 23.67, 22.74, 14.21.

4.1.2. Synthesis of polymers

General procedures of Suzuki copolymerization, taking PFO-SO as an example.

Under an argon atmosphere, a solution of **M3** (321.28 mg, 0.5 mmol), **M4** (268.73 mg, 0.49 mmol), **M2** (7.63 mg, 0.01 mmol) and toluene was added to palladium acetate ($Pd(OAc)_2$) (3.4 mg, 0.015 mmol) and tricyclohexyl-phosphine (PCy_3) (8.4 mg, 0.03 mmol). The reaction mixture was stirred and heated up to 80 °C. After the mixture became clear, tetraethyl ammonium hydroxide (Et_4NOH) (20% aq, 2 mL) was added. The temperature was kept in the range of 80–85 °C, and the solution was allowed to stir vigorously for 36 h. The reaction was end-capped by adding phenylboronic acid (0.05 g, 0.4 mmol) and was allowed to stir for 12 h. Then bromobenzene (0.125 g, 0.8 mmol) was added followed by stirring for another 12 h. After cooling, the mixtures were precipitated into methanol (150 mL) and filtered. The collected solids were re-dissolved in dichloromethane and washed three times with de-ionized water. The organic phase was concentrated under reduced pressure, followed by re-precipitation in methanol. The crude product was further purified by Soxhlet extraction by methanol and acetone successively. The target polymer was collected after drying under vacuum with a yield of 60%. ^{1}H NMR (500 MHz, $CDCl_3$) δ (ppm) 7.85–7.84 (br, ArH), 7.71–7.68 (br, ArH), 2.21 (br, CH_2), 1.22–1.44 (br, CH_2), 0.83–0.80 (br, CH_3).

PFO. M3 (321.28 mg, 0.5 mmol) and **M4** (274 mg, 0.5 mmol), yield: 76%. ^{1}H NMR (500 MHz, $CDCl_3$) δ (ppm) 7.85–7.84 (br, ArH), 7.71–7.68 (br, ArH), 2.21 (br, CH_2), 1.20–1.440 (br, CH_2), 0.83–0.80 (br, CH_3).

PFO-Cz. M3 (321.28 mg, 0.5 mmol), **M4** (268.73 mg, 0.49 mmol), **M1** (7.13 mg, 0.01 mmol), yield: 70%. ^{1}H NMR (500 MHz, $CDCl_3$) δ (ppm) 7.85–7.84 (br, ArH), 7.71–7.68 (br, ArH), 2.23–2.21 (br, CH_2), 1.45–1.30 (br, CH_2), 0.83–0.80 (br, CH_3).

4.2. Measurements

Nuclear magnetic resonance (NMR) spectra were recorded on a Bruker DRX 500 spectrometer (operating at 500 MHz for ^{1}H NMR, and 125 MHz for ^{13}C NMR) in deuterated chloroform solution. Tetramethylsilane was used as the reference. The X-ray diffraction (XRD) were studied by a Bruker D8 Advance diffractometer equipped with a copper target (Kα line, with wavelength $\lambda = 0.154$ nm). Cyclic voltammetry (CV) was measured by using a CHI660A electrochemical work-station. The measurement was performed at a scan rate of 50 mV s^{-1} at room temperature under the inert atmosphere of Ar. The tetra-(*n*-butyl)ammonium hexafluorophosphate (n-Bu_4NPF_6, 0.1 M) in acetonitrile solution was selected as the electrolyte. Differential scanning calorimetry (DSC) measurements were carried out on a Netzsch DSC 204 at a heating rate of 10 °C min^{-1} under N_2. Thermal gravimetric analysis (TGA) was carried out in a NETZSCH TGA-209 thermal analyzer. All measurements were carried out under N_2 with a heating rate of 20 °C min^{-1}. UV–vis absorption spectra of polymers in both dilute toluene solution and as thin films were recorded with a HP 8453 spectrophotometer. Photoluminescence (PL) spectra were recorded with a Spex Fluorolog-3 spectrofluorometer.

The fabrication of the devices followed a well-established process. The ITO glass substrates with sheet resistance of 15–20 Ω/square were successively cleaned in an ultrasonic bath by using acetone, detergent, deionized water, and isopropanol. The ITO glass subtracts were dried over 12 h at 80 °C. A PEDOT:PSS layer, with thickness of about 40 nm was spin-coasted onto the ITO substrate, which has been treated by oxygen plasma. Then the PEDOT:PSS film was heated at 120 °C for 20 min. These light-emitting polymers were spin-coated from *p*-xylene solution on the top of the preformed PEDOT:PSS layer, and then the resulting films were annealed at 100 °C on a hotplate for 20 min. The thickness of the emissive layer was determined by a Tencor Alpha-step 500 Surface Profilometer. For the cathode 1.5 nm of CsF followed by 120 nm of aluminum (thickness monitored with a STM–100/MF Sycon quartz crystal) were deposited by thermally evaporating at a base pressure of 1×10^{-6} Pa. The pixel area (16 mm^2) was defined by a shadow mask between the cathode and anode. Except for the deposition of PEDOT:PSS layer, all other procedures were carried out in the nitrogen filled glove-box with the oxygen and moisture below 10 ppm. The PLEDs were encapsulated with a UV-cured epoxy resin.

The current density (J) – voltage (V) – luminance (L) characteristics were collected by using a Keithley 236 source measurement unit. The system was calibrated by silicon photodiode before use. The external quantum efficiency of electroluminescence was recorded by measuring the total light output in all directions in an integrating sphere with calculated photodiodes (IS-080, Labsphere). The luminance was calibrated by using a PR-705 Spectra Scan Spectro-photometer (Photo Research), with simultaneous acquisition of the EL spectra and CIE coordinates, driven by a Keithley model 2400 voltage-current source. The morphology of the polymer film was characterized by a tapping mode atomic force microscopy (AFM), which consists a Seiko SPA 400 equipped with an SPI 3800 probe station.

Acknowledgements

The authors are grateful for financial support from the Ministry of Science and Technology-China (2016YFB0401302 and 2015CB655004), and the National Natural Science Foundation of China (Grants 51303056, 51473054 and 51273069).

Appendix A. Supplementary data

Supplementary data related to this article can be found at http://dx.doi.org/10.1016/j.orgel.2016.08.007.

References

[1] L.H. Xie, C.R. Yin, W.Y. Lai, Q.L. Fan, W. Huang, Polyfluorene-based semiconductors combined with various periodic table elements for organic electronics, Prog. Polym. Sci. 37 (2012) 1192–1264.

[2] L. Ying, C.L. Ho, H.B. Wu, Y. Cao, W.Y. Wong, White polymer light-emitting devices for solid-state lighting: materials, devices, and recent progress, Adv. Mater 26 (2014) 2459–2473.

[3] B.H. Zhang, G.P. Tan, C.-S. Lam, B. Yao, C.-L. Ho, L.H. Liu, Z.Y. Xie, W.-Y. Wong, J.Q. Ding, L.X. Wang, High-efficiency single emissive layer white organic light-emitting diodes based on solution-processed dendritic host and new orange-emitting iridium complex, Adv. Mater 24 (2012) 1873–1877.

[4] L. Ying, J.H. Zou, W. Yang, A.Q. Zhang, Z.L. Wu, W. Zhao, Y. Cao, Novel, blue light-emitting polyfluorenes containing a fluorinated quinoxaline unit, Dyes Pigments 82 (2009) 251–257.

[5] T. Guo, L. Yu, B.F. Zhao, L. Ying, H.B. Wu, W. Yang, Y. Cao, Blue light-emitting hyperbranched polymers using fluoreneco-dibenzothiophene-*S,S*- dioxide as branches, J. Poly. Sci. Poly. Chem. 53 (2015) 1043–1051.

[6] L.W. Hu, Y. Yang, J. Xu, J.F. Liang, T. Guo, B. Zhang, W. Yang, Y. Cao, Blue light-emitting polymers containing fluorene based benzothiophene-*S,S*-dioxide derivatives, J. Mater. Chem. C 4 (2016) 1305–1312.

[7] X.C. Wang, L. Zhao, S.Y. Shao, J.Q. Ding, L.X. Wang, X.B. Jing, F.S. Wang, Poly(spirobifluorene)s containing nonconjugated diphenylsulfone moiety: toward blue emission through a weak charge transfer effect, Macromolecules 47 (2014) 2907–2914.

[8] S.H. Chen, A.C. Su, C.H. Su, S.A. Chen, Crystalline forms and emission behavior of poly(9,9-di-n-octyl-2,7-fluorene), Macromolecules 38 (2005) 379–385.

[9] S.K. Lee, T. Ahn, N.S. Cho, J.-I. Lee, Y.K. Jung, J. Lee, H.K. Shim, Synthesis of new polyfluorenecopolymers with a comonomercontaining triphenylamineunits and their applications in white-light-emitting diodes, J. Polym. Sci. Part A Polym. Chem. 45 (2007) 1199–1209.

[10] Y. Yang, L. Yu, Y. Xue, Q.H. Zou, B. Zhang, L. Ying, W. Yang, J.B. Peng, Y. Cao, Improved electroluminescence efficiency of polyfluorenes by simultaneously incorporating dibenzothiophene-*S,S*-dioxide unit in main chain and oxadiazole moiety in side chain, Polymer 55 (2014) 1698–1706.

[11] K.M. Schelkle, M. Bender, K. Jeltsch, T. Buckup, K. Mîllen, M. Hamburger, U.H.F. Bunz, Light-induced solubility modulation of polyfluorene to enhance the performance of OLEDs, Angew. Chem. Int. Ed. 54 (2015) 14545–14548.

[12] K.L. Chan, M. Sims, S.I. Pascu, M. Ariu, A.B. Holmes, D.D.C. Bradley, Understanding the nature of the states responsible for the green emission in oxidized poly(9,9-dialkylfluorene)s: photophysics and structural studies of linear dialkylfluorene/fluorenone model compounds, Adv. Funct. Mater 19 (2009) 2147–2154.

[13] J. Peet, E. Brocker, Y.H. Xu, G.C. Bazan, Controlled β-phase formation in poly(9,9-di-*n*-octylfluorene) by processing with alkyl additives, Adv. Mater 20 (2008) 1882–1885.

[14] M. Knaapila, A.P. Monkman, Methods for controlling structure and photophysical properties in polyfluorene solutions and gels, Adv. Mater 25 (2013) 1090–1108.

[15] W.C. Tsoi, A. Charas, A.J. Cadby, G. Khalil, A.M. Adawi, A. Iraqi, B. Hunt, J. Morgado, D.G. Lidzey, Observation of the β-phase in two short-chain oligofluorenes, Adv. Funct. Mater 18 (2008) 600–606.

[16] D.W. Bright, F.B. Dias, F. Galbrecht, U. Scherf, A.P. Monkman, The influence of alkyl-chain length on beta-phase formation in polyfluorenes, Adv. Funct. Mater 19 (2009) 67–73.

[17] E.D. Como, N.J. Borys, P. Strohriegl, M.J. Walter, J.M. Lupton, Formation of a defect-free π-electron system in single β-phase polyfluorene chains, J. Am. Chem. Soc. 133 (2011) 3690–3692.

[18] X.W. Zhang, Q. Hu, J.Y. Lin, Z.F. Lei, X. Guo, L.H. Xie, W.Y. Lai, W. Huang, Efficient and stable deep blue polymer light-emitting devices based on beta-phase poly(9,9-dioctylfluorene), Appl. Phys. Lett. 103 (2013) 153301.

[19] J.F. Liang, W.K. Zhong, L. Ying, W. Yang, J.B. Peng, Y. Cao, The effects of solvent vapor annealing on the performance of blue polymer light-emitting diodes, Org. Electron 27 (2015) 1–6.

[20] K. Zhao, G. Zhou, Q. Wang, Y.C. Han, L.X. Wang, D.G. Ma, Phase separation in poly(9,9-dioctylfluoxene)/poly(methyl methacrylate) blends, Macromol. Chem. Phys. 211 (2010) 313–320.

[21] M.C. Hung, J.L. Liao, S.A. Chen, S.H. Chen, A.C. Su, Fine tuning the purity of blue emission from polydioctylfluorene byend-capping with electron-deficient moieties, J. Am. Chem. Soc. 127 (2005) 14576–14577.

[22] S.K. Lee, T. Ahn, J.H. Park, Y.K. Jung, D.S. Chung, C.E. Parke, H.K. Shim, β-Phase formation in poly(9,9-di-*n*-octylfluorene) by incorporating an ambipolar unit containing phenothiazine and 4-(dicyanomethylene)-2-methyl-6-[*p*-(dimethylamino) styryl]-4*H*-pyran, J. Mater. Chem. 19 (2009) 7062–7069.

[23] W.C. Tsoi, A.R. Buckley, D.G. Lidzey, Probing the transitions between morphological phases in an oligofluorene thin-film using temperature-dependent photoluminescence spectroscopy, Chem. Phys. Lett. 468 (2009) 32–36.

[24] T. Shiraki, S. Shindome, F. Toshimitsu, T. Fujigayaa, N. Nakashima, Strong main-chain length-dependence for the β-phase formation of oligofluorenes, Polym. Chem. 6 (2015) 5103–5109.

[25] J.Y. Lin, W.S. Zhu, F. Liu, L.H. Xie, L. Zhang, R.D. Xia, G.C. Xing, W. Huang, A rational molecular design of β-phase polydiarylfluorenes: synthesis, morphology, and organic lasers, Macromolecules 47 (2014) 1001–1007.

[26] J.F. Liang, L. Yu, S. Zhao, L. Ying, F. Liu, W. Yang, J.B. Peng, Y. Cao, Improving efficiency and color purity of poly(9,9-dioctylfluorene) through addition of a high boiling-point solvent of 1-chloronaphthalene, Nanotechnology 27 (2016) 284001.

[27] J.A. Mikroyannidis, H.A. Moshopoulou, J.A. Anastasopoulos, M.M. Styllanakis, L. Fenenko, C. Adachi, A glass-forming conjugated main-chainliquid crystal polymerfor polarized electroiuminescence applications, J. Polym. Sci. Polym. Chem. 44 (2006) 6790–6800.

[28] S.H. Chen, A.C. Su, Noncrystalline phases in poly(9,9-di-*n*-octyl-2,7-fluorene), J. Phys. Chem. B 109 (2005) 10067–10072.

[29] H.H. Lu, C.Y. Liu, C.H. Chang, S.A. Chen, Self-dopant formation in poly(9,9-di-*n*-octylfluorene) via a dipping method for efficient and stable pure-blue electroluminescence, Adv. Mater 19 (2007) 2574–2579.

[30] Y.Y. Li, H.B. Wu, J.H. Zou, L. Ying, W. Yang, Y. Cao, Enhancement of spectral stability and efficiency on blue light-emitters via introducing dibenzothiophene-*S,S*-dioxide isomers into polyfluorene backbone, Org. Electron 10 (2009) 901–909.

[31] T. Guo, L. Yu, Y. Yang, Y.H. Li, Y. Tao, Q. Hou, L. Ying, W. Yang, H.B. Wu, Y. Cao, Hyperbranched red light-emitting phosphorescent polymers based on iridium complex as the core, J. Lumin 167 (2015) 179–185.